UNIDIRECTIONAL ANISOTROPY IN MANGANITE BASED FERROMAGNETIC-ANTIFERROMAGNETIC MULTILAYERS

I. PANAGIOTOPOULOS[1], C. CHRISTIDES[2],
M. PISSAS[1], AND D. NIARCHOS[1]
1. Institute of Materials Science, NCSR "Demokritos", Ag. Paraskevi Attiki, 153 10 Greece
2. Department of Engineering Sciences, School of Engineering University of Patras, 26110 Patras, Greece

1. Introduction

In mixed valence manganites a large negative magnetoresistance (MR), termed colossal magnetoresistance [1] (CMR), can be obtained due to a metal-insulator transition at the ferromagnetic Curie point [2]. However little progress has been made towards using these materials in applications, mainly due to the strong temperature dependence of the CMR effect and the large saturation fields (of the order of Tesla) required. Tunneling and grain boundary effects [3-8] as well as interface scattering [9] seem promising towards getting useful MR in these materials. In particular the high degree of spin polarization [10] makes these materials promising for spin-electronic device applications.

In view of the above considerations, recently several publications have focused on the study of trilayers and multilayers based on mixed valence manganites [11-20]. The magnetic and magnetotransport properties of such structures are not a mere superposition of the response of the individual layers. This is a result of possible interface scattering [11-17], interlayer interactions [19,20] and stress effects due to lattice mismatch between the layers [11,12,14,16].

The sensitivity of double exchange and superexchange interactions to Mn-O bond lengths and Mn-O-Mn bond angles has been used as a structural tuning mechanism of magnetic and MR properties in bulk CMR manganites [21,22]. Such changes can be engineered through various substitutions that alter the configuration of Mn-O octahedra. In epitaxial thin films, strain due to lattice mismatch can give rise to structural deformations. Thus, depending on the substrate used, the film can be under ductile or tensile strain that results in changes of magnetic anisotropy and MR properties [23-27].

In what follows we report on the magnetic structural and MR properties of $La_{2/3}Ca_{1/3}MnO_3/La_{1/3}Ca_{2/3}MnO_3$ multilayers showing exchange biasing effects. The $La_{2/3}Ca_{1/3}MnO_3$ layers are ferromagnetic (FM) and $La_{1/3}Ca_{1/3}MnO_3$ layers are antiferromagnetic (AF) [28]. The structural compatibility of the AF and FM layers permits coherent growth of the superlattices that satisfy the conditions for magnetic coupling at the interfaces.

G.M. Chow et al. (eds.), Nanostructured Films and Coatings, 177–185.

The existence of unidirectional anisotropy due to exchange coupling between a FM and an AF phase was first reported in oxide-coated fine particles of Co [29]. The exchange anisotropy results in a displaced magnetic hysteresis loop when the sample is field cooled through the Néel temperature of the AF phase. In early studies, this loop displacement has been explained by assuming an ideal FM/AF interface with uncompensated moments in the atomic-plane of the AF layer at the FM/AF boundary [29]. Up to date exchange anisotropy effects have been studied mainly in AF/FM systems consisting of transition metal alloys and metallic oxides (e.g. FM= Co, NiFe, Fe_3O_4, and AF=CoO, FeMn) [30], but not in manganites where the magnetic interactions cannot be described by direct-exchange.

2. Experimental details

The films were deposited on (001) $LaAlO_3$ substrates by pulsed laser deposition (PLD) from bulk stoichiometric $La_{2/3}Ca_{1/3}MnO_3$ target samples. The targets were prepared by standard solid state reaction from La_2O_3, $CaCO_3$ and MnO_2 powders sintered at 1300^0C for 5 days with two intermediate grindings. MR measurements were performed with a four-probe method and with the current parallel to the applied magnetic field. The θ-2θ X-ray diffraction data were obtained with a Siemens D500 diffractometer using $Cu_{K\alpha}$ radiation and a secondary graphite monochromator. The magnetic measurements were performed in a SQUID magnetometer (Quandum Design). A series of $La_{2/3}Ca_{1/3}MnO_3/La_{1/3}Ca_{2/3}MnO_3$ multilayers with equal AF (t_{AF}) and (t_{FM}) FM layer thickness and bilayer thickness (Λ) ranging from 2 to 32 nm were grown along the (001) direction of the simple pseudocubic perovskite unit cell. The structural compatibility of the AF and FM layers permits coherent growth that favors magnetic coupling. In order to deposit in a multilayer form, the targets were mounted on a step-motor controlled rotatable carrier that allows the $La_{2/3}Ca_{1/3}MnO_3$ and $La_{1/3}Ca_{2/3}MnO_3$ targets to be sequentially exposed in the beam path. The substrate was located at a distance of 6 cm from the target, by the edge of the visible extent of the plume. The substrate temperature (Ts) was 700^0C and the oxygen pressure in the chamber during the deposition was 0.03 Torr. The resulting rate at fluence of 1.5 J/cm^2 on the target was 0.4 Å/pulse.

3. Structural Characterization

The existence of the superstructure has been confirmed from the presence of low-angle superlattice Bragg-peaks and multiple satellite peaks around the (001), (002) and (003) Bragg-reflections of the constituents. In the low angle diffraction patterns the even order satellites are not observed due to the $t_{AF}=t_{FM}=\Lambda/2$ condition.

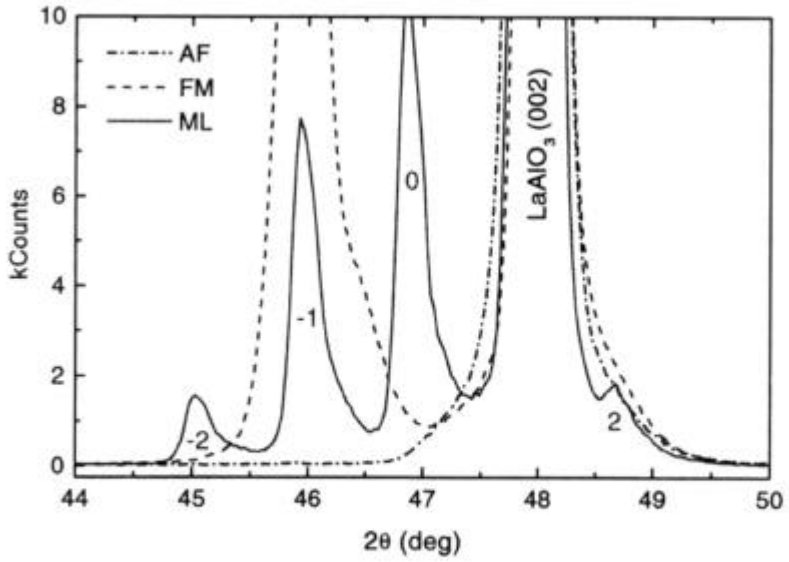

Figure 1. The XRD pattern of a multilayer sample compared to those of single AF and FM layers.

The main Bragg peak lies between the Bragg peaks observed in single AF and FM layer films and is surrounded by satellite peaks due to the layered structure (Fig.1). The existence of an average Bragg peak for $\Lambda \leq 10$nm indicates that for this range of bilayer thickness we have a coherent layer growth. The values of Λ were estimated by the formula $\Lambda = n\lambda_{Cu}/2(\sin\theta_n - \sin\theta_0)$ where θ_n are diffraction angles of the n-th order satellite and θ_0 is the average Bragg peak. The (00ℓ) LAO Bragg-peaks (ℓ=1,2, and 3) interfere with the satellite peaks adjacent to the fundamental (zeroth order) peaks of the multilayer, introducing uncertainties in the quantitative analysis of the XRD spectra. Asymmetric intensity of the satellite peaks has been reported in multilayers in which a chemical and/or strained interfacial profile is assumed along the growth direction of the superlattice. Since for all the examined Λ values there are no traces of mixed (001) and (110) textures, cumulative roughness effects resulting to extra surface roughness and mosaic spread with increasing Λ can be excluded.

4. Magnetization and Magnetoresistance Measurements

Magnetic hysteresis loops, measured at 10 K after cooling down from 300 K in zero field (ZFC) and in 10 kOe (FC), for a $LaAlO_3$/[FM(5 nm)/AF(5 nm)]$_{15}$ sample are shown in Fig.2. It is evident that the ZFC loop is symmetric around the zero field, while the FC loop is shifted towards negative fields. This effect can be attributed to exchange biasing at the AF/FM interface, since single-layered FM films do not exhibit any loop displacement after the FC process. If H_1 is the lower and H_2 is the higher field value where the average film magnetization becomes zero, then the exchange biasing field is

defined as the loop shift $H_{EB}= -(H_1+H_2)/2$ and the coercivity as the halfwidth of the loop $H_C=(H_1-H_2)/2$. Thus, we calculate for the FC loop an H_{EB}=880 *Oe*, and a H_C=800 *Oe* which is almost double compared to the H_C value obtained from the ZFC loop. Additional magnetic measurements were performed in order to investigate the origin of this effect. The temperature dependence of H_{EB} and H_C values is shown in

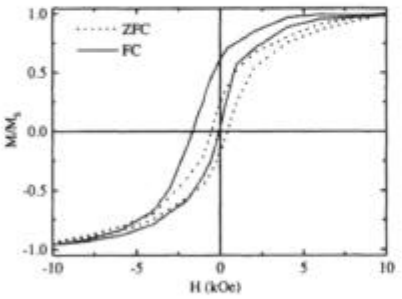

Figure 2. Hysteresis loops, measured at 10 K after cooling down from 300 K in zero field (ZFC) and in 10 kOe (FC), fo the Λ=10 nm multilayer.

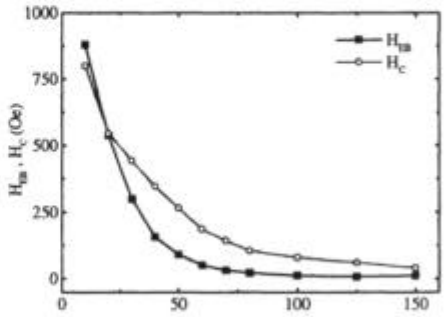

Figure 3. Temperature dependence of exchnage biasing field (H_{EB}) and coercive field (H_C) for Λ=10 nm multilayer.

Fig.3. These values were estimated from isothermal loops measured in constant temperature intervals, after FC the sample from 300 K down to 10 K in 10 k*Oe* and then warming up. It is evident that H_{EB} decreases and disappears around the blocking temperature T_B of 70 K. The H_C values exhibit a similar trend, indicating a connection between the mechanisms that give rise to coercivity and loop displacement. The excess coercivity observed below T_B is induced by random exchange fields at the AF/FM interfaces. This low-temperature anisotropy can be treated as an additional energy barrier in the magnetic free energy, as in the case of superparamagnetic particles [23].

Since exchange biasing is an interface related phenomenon a strong dependence on the individual FM and AF layer thickness is expected. The maximum H_{EB} is observed for the sample with Λ=10 nm. H_C follows the variation of H_{EB} with Λ, indicating that there is a significant contribution in H_C from the exchange anisotropy at the AF/FM interfaces. A decrease of H_{EB} at higher Λ is observed as expected due to the decreased contribution of the interfaces. However H_{EB} also decreases at lower Λ due to the decreased contribution of the AF layers.

Additional magnetic measurements were performed in order to investigate the origin of this effect. In Fig.4 the ZFC and FC measurements of the magnetization, normalized to the total FM volume of the sample, are shown for the above series of multilayers as a function of temperature. Both measurements were performed by warming up in 1 kOe after having cooled in zero field and 10 kOe respectively. The ZFC and FC curves coincide at temperatures higher than 100 K and become zero at about 250 K, where the Curie point T_C of the FM layers is expected. The ZFC curve exhibits a broad peak around the T_B 70 K, whereas the FC curve exhibits a steep increase just below T_B. It is reasonable to assume that in the FC measurement an increase of magnetization results from the alignment of interfacial magnetic moments, giving rise to unidirectional

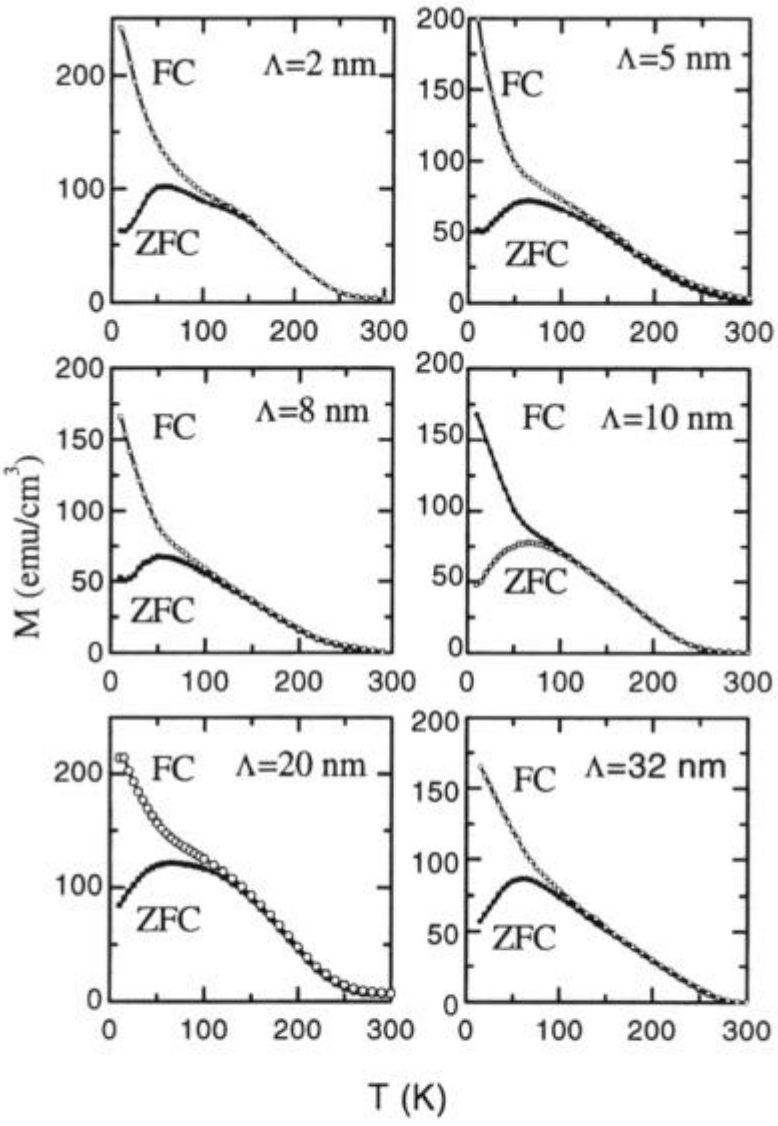

Figure 4. Magnetization as a function of temperature for the series of $[FM(\Lambda/2nm)/AF(\Lambda/2nm)]_{15}$ multilayers. The measurements were performed by warming up in 1 kOe after having cooled down to 10 K, in zero field (ZFC) and 10 kOe (FC) respectively.

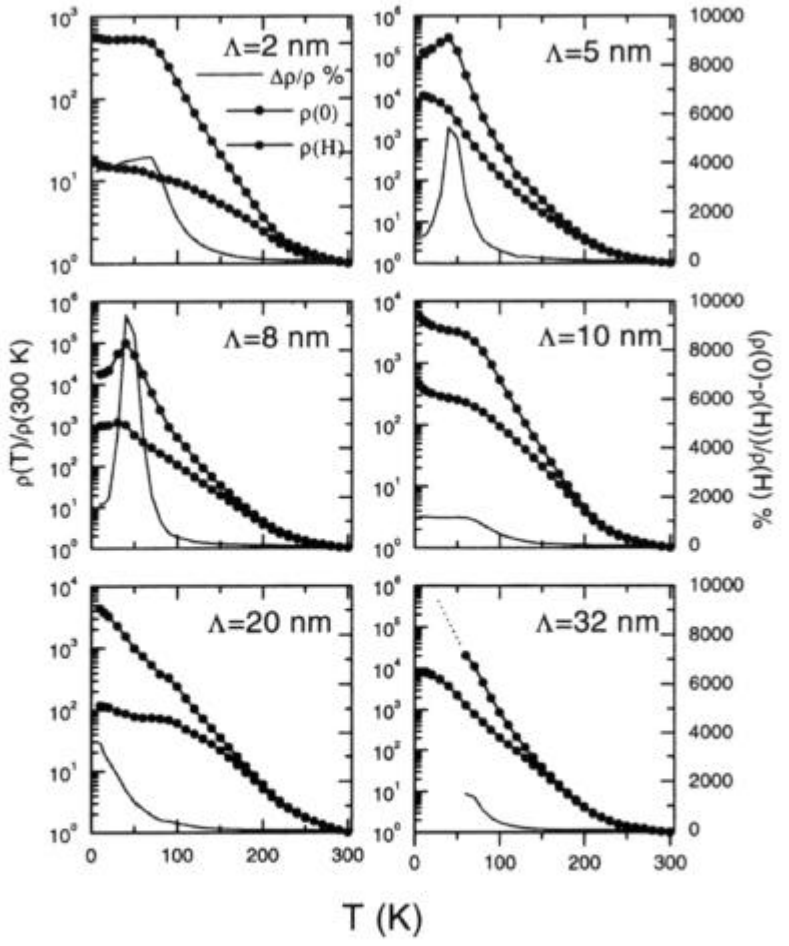

Figure 5. Resistivity, normalized to the 300 K value, as a function of temperature, measured in 50 kOe (ρ_H) and in zero applied field (ρ_0) for the series of $[FM(\Lambda/2)/AF(\Lambda/2)]_{15}$ multilayers. The CMR ratio $\Delta\rho/\rho_H=[\rho_0-\rho_H]/\rho_H$ is plotted as a solid line.

anisotropy [16] below T_B. Hence, the observed hump below T_B in the ZFC curve can be attributed to thermally activated magnetic rotation over energy barriers caused by random exchange coupling at the AF/FM interfaces. Our magnetothermal measurements indicate that the T_B does not change in the examined range of bilayer thickness and occurs at 70 K for all samples. To answer why T_B remains more or less the same in the examined range of Λ values it is reasonable to consider that interfacial spin ordering is confined within a few atomic planes near the AF/FM interfaces, defining an active film volume V_{int}. Thus, the appearance of exchange-biasing depends on the magnetic ordering of interfacial atomic planes which define a critical volume where thermal-activation energy becomes comparable to the magnetic energy at a certain blocking temperature, independent of Λ. Figure 5 shows the variation of the normalized resistivity as a function of temperature, measured in 50 kOe (ρ_H) and in zero applied field (ρ_0). The resistivity increases drastically as we cool down from 300 K, spanning almost four orders of magnitude. Also, the CMR ratio becomes maximum in the temperature range below T_B. In Fig.5 the steep increase of resistivity at low temperatures is in contrast to the decrease of ρ observed in epitaxial FM films [24,25]. This provides further experimental evidence that the insulating behavior [26] of the AF layer is dominant at low-temperatures. This extra contribution in ρ is different for every specimen and modifies the shape of the resultant CMR curves (Fig.6). Clearly, the multilayers with Λ=5 and 8 nm exhibit a peak in the CMR response, indicating a special arrangement of spins at the AF/FM interfaces. As a consequence the characteristic CMR peak, that is usually reported nearby the ferromagnetic T_C of $La_{2/3}Ca_{1/3}MnO_3$ films [27] is not observed in the ρ_0 versus temperature curve. This behavior is in agreement with the magnetothermal measurements (Fig.5), where it is evident that the most drastic change of the average film magnetization does not occur near the T_C of the individual FM layers but at T_B.

5. Conclusion

In summary, we have studied the variation of exchange biasing and coercive field as a function of Λ and temperature in $La_{2/3}Ca_{1/3}MnO_3/La_{1/3}Ca_{2/3}MnO_3$ multilayers grown by PLD. The maximum H_{EB}=880 Oe was observed for the sample with Λ=10 nm. The exchange biasing mechanism sets-in below a blocking temperature of 70 K and induces: (i) an enhancement of H_C in the FC hysteresis loops, (ii) an increase of the MR ratio due to interface scattering around T_B. It is interesting to note that in the series of multilayers studied here despite all variations in the AF and FM layer thicknesses T_B does not vary considerably, signifying that the mechanism of spin ordering is confined within a few atomic planes near the AF/FM interfaces. This may be attributed to weak coupling of the interfacial spins to the core of the AF layer.

References

1. Jin, S., Tiefel, T.H., McCormack, M., Fatsnacht, R.A., Ramesh, R. Chen, L.H. (1994) Thousandfold change in resistivity in magnetioresistive La-Ca-Mn-O films, *Science* **264**, 413-415
2. Radaelli, P.G., Cox, D.E., Maresio, M., Cheong, S-W., Schiffer, P.E., and Ramirez, A.P. (1995) Simultaneous Structural, Magnetic, and Electronic Transitions in $La_{1-x}Ca_xMnO_3$ with x=0.25 and x=0.50, *Phys. Rev. Lett.* **75**, 4488-4491
3. Yu Lu, Li, X.W., Gong, G.Q., Gang Xiao, Gupta, A., Lecoeur, P., Sun, J.Z., Wang, Y.Y. and Dravid, V.P. (1996) Large magnetotunneling effect at low magnetic fields in micrometer scale epitaxial $La_{0.67}Sr_{0.33}MnO_3$ tunnel junctions *Phys. Rev.* B**54**, R8354-8360
4. Mathur, N.D., Burnell, G., Isaac, S.P., Jackson, T.J., Teo, B.-S., MacManus-Driscoll, J.L., Cohen, L.F. Evetts, J.E. and Balmire, M.G. (1997) Large low field magnetoresistance in LaCaMnO induced by artificial grain boundaries, *Nature* **387**, 266-268.
5. Steenbeck, K., Eick, T., Krisch, K., Schmidt, H-G., and Steinbeissh, E., (1998) Tunneling-like magnetoresistance in bicrystal LaSrMnO thin films, *Appl. Phys. Lett.* **73**, 2506-2508.
6. Srinitiwarawong, C.,and Ziese, M. (1998) Magnetoresistance of mechanically induced grain boundaries in LaCaMnO films, *Appl. Phys. Lett.* **73**, 1140-1142.
7. Ziese, M. (1999) Grain-boundary magnetoresistance: Spin-polarized inelastic tunneling through spin-glass-like barrier, *Phys. Rev.* B**60**, R738-R741.
8. Coey, J.M.D. (1999) Powder Magnetoresistance *J. Appl. Phys.* **85**, 5576-5581.
9. Ziese, M., Sena, S., Shearwood, C., Blythe, H.J., Gibbs, M.R.J., Gehing, G.A. (1998) Voltage-controlled colossal magnetoresistance in manganite/normal-metal heterostructures *Phys. Rev.* B**57**, 2963-2967
10. Wei, J.Y.T., Yeh, N.-C. Vasquez, R.P., Gupta, A., (1998) Tunneling evidence of half-metallicity in epitaxial films of ferromagnetic perovskite manganites and ferrimagnetic mangetite, *J. Appl. Phys.* **83**, 7366-7368
11. Gong, G.Q., Gupta, A., Gang Xiao, Lecoeur, P., and, McGuire, T.R., (1996) Perovskite oxide superlattices: magnetotransport and magnetic properties *Phys. Rev.* B**54**, R3742-3745.
12. Kwon, C., Kim, K.-C., Robson, M.C., Gu, J.Y., Rajeswari, M., Venkatesan T, and. Ramesh, R.(1997) Desirable magnetotransport properties in doped Mn-oxide-based superlattices *J.Appl. Phys.* **81**, 4950–4952
13. Ghosh, K. Ogale, S.B,. Pai, S.P, Robson, M., Eric Li, Jin, I., Zi-Wen Dong, Greene, R.L., Ramesh, R., Venkatesan, T., and Johnson, M., (1998) Positive giant magnetoresistance in a $Fe_3O_4/SrTiO_3$ /$La_{0.7}Sr_{0.3}MnO_3$ heterostructure *Appl. Phys. Lett.* **73**, 689-691.
14. Rongsheng Cheng, Kebin Li, Shouguo Wang, Zhixiang Chen, Caoshui Xiong, Xiaojun Xu and Yuheng Zhang, (1998). The special magnetoresistive effect in trilayered films of manganite perovskites, *Appl. Phys. Lett.* **72**, 2475-2477.
15. Sun, J.Z., Abraham, D.W., Roche, K., and Parkin, S.S.P. (1998) Temperature and bias dependence of magnetoresistance in doped manganite thin film trilayer junctions, *Appl. Phys. Lett.* **73**, 1008-1010.
16. Wiedenhorst, B., Hoefener, C., Yafeng Lu, Klein, J., Alff, L. Gross, R. Freitag, B.H. Mader, W. (1999) Strain effects and microstructure of epitaxial manganite thin films and heterostructures, *Appl. Phys. Lett.* **74**, 3636-3638
17. .Sahana, M, Hedge, M.S., Prasad, V., and Subamanyam, S.V. (1999) Electrical resistivity and enhanced magnetoresistance in LaPbMnO/LaMnO superlattices *J. Appl. Phys.* **85**, 1058-1061
18. Panagiotopoulos, I., Christides, C., Pissas, M., and Niarchos, D.(1999) Exchange biasing mechanism in $La_{2/3}Ca_{1/3}MnO_3$/ $La_{1/3}Ca_{2/3}MnO_3$ multilayers *Phys. Rev.* B **60**, 485-491
19. Izumi, M., Murakami, Y., Konishi, Y., Manako, T., Kawasaki, M., Tokura, Y., (1999) Structure characterization and magnetic properties of oxide superlattices LaSrMnO/LaSrFeO *Phys. Rev.* B**60**, 1211-1215.
20. Nikolaev, K.R., Bhattachrya A., Kraus, P.A., Vas'ko, V.A., Cooley, W.K., and Goldman, A.M., (1999) Indications of antiferromagnteic interlayer coupling in $La_{2/3}Ba_{1/3}MnO_3/LaNiO_3$ multilayers *Appl. Phys. Lett.* **75**,118-120
21. Fontcuberta J., Martinez, B., Seffar, A., Pinol S., Garcia-Munoz, J.L. and Obradors, X. (1997) Colossal magnetoresistance of ferromagnetic manganites: Structural tuning and mechanisms *Phys. Rev. Lett.* **76**, 1122-1125.
22. Kuwahara, H., Moritomo, Y., Tomioka, Y., Asamitsu, A., Kasai, M. and Tokura, Y. (1997) Low-field colossal magnetoresistance in bandwidth-controlled manganites *J. Appl. Phys.* **81**, 4954-4957
23. Koo T.Y., Park, S.H. Lee K-B., Jeong, Y.H. (1997) Anisotropic strains and magnetoresistance of $La_{0.7}Ca_{0.3}MnO_3$ *Appl. Phys. Lett.* **71**, 977-979

24. Wang H. S. and Qi Li, (1998).Strain-induced large low-field magnetoresistance in $Pr_{0.67}Sr_{0.33}MnO_3$ ultrathin films *Appl. Phys. Lett.* **73**, 2360-2362
25. O'Donnel, J. Rzchowski, M.S. Eckstein, J.N. and Bozovic, I. (1998).Magnetoelastic coupling and magnetic anisotropy in LaCaMnO films *Appl. Phys. Lett.* **72**, 1775-1777
26. Wang, H. S. Qi Li, Kai Liu and Chien, C.L. (1999).Low-field magnetoresistance and anisotropy in ultrathin PrSrMnO films grown on different substrates *Appl. Phys. Lett.* **74**, 2212
27. Nath, T. K. Rao, R. A. Lavric, D. Eom, C. B. Wu, L. and Tsui, F. (1998).Effect of three-dimensional strain states on magnetic anisotropy of LaCaMnO epitaxial thin films *Appl. Phys. Lett.* **73**, 1615-1617
28. Millis, J. (1998) Lattice effects in magnetoresistive manganese perovskites *Nature* **392**, 147-150
29. Meiklejohn, W. H. and Bean, C. P. (1957) New Magnetic Anisotropy *Phys. Rev.* **105**, 904 -913
30. For a recent review on Exchange Biasing phenomena see Nogues, J. and Schuller, Ivan K. (1999) Exchange Bias *J. Magn. Magn. Mat.* **192**, 203-232